

Selection of the Taylor-Saffman Bubble without Surface Tension

Giovani L. Vasconcelos

Laboratório de Física Teórica e Computacional, Departamento de Física,
Universidade Federal de Pernambuco, 50670-901, Recife, Brazil.

Mark Mineev-Weinstein

New Mexico Consortium, Los Alamos, NM 87544, US

(Dated: October 23, 2019)

By presenting the most general to date class of exact solutions, we demonstrate that the attractor for zero surface tension non-singular bubble dynamics in a Hele-Shaw cell is the selected pattern.

Introduction. Steady patterns, often observed in various unstable non-equilibrium systems, are formed, as a rule, after a transient nonlinear interface dynamics between two phases. The problem of selecting a single observed pattern from a continuum of possible solutions, such as a parabolic dendrite in supercooled liquid [1] and a finger in a Hele-Shaw cell [2], attracted considerable attention in the past (see details in [3]). Besides the obvious importance for non-equilibrium physics, the interest was heated up by mathematical difficulties to include surface tension, considered indispensable for the selection. These difficulties were resolved in [4], and it was shown that surface tension indeed selects the pattern. More recently, analysis of exact solutions for the interface dynamics in a Hele-Shaw channel demonstrated that selection of the observed finger [2] is possible without surface tension [5]. The present work significantly extends this result by addressing the bubble dynamics instead of a finger.

The pattern selection problem for an inviscid bubble dragged by a viscous flow in a narrow gap between parallel plates (Hele-Shaw cell) was posed by Taylor and Saffman in 1959 [6] and was later addressed experimentally [7] and theoretically [8]. To be specific, the problem was how to select, from the continuum of steady state solutions obtained for zero surface tension, the unique bubble [6] with velocity, twice the background flow velocity in the limit of low surface tension. While it has long been known that the inclusion of surface tension leads to velocity selection [8], we demonstrate in this paper that the selection mechanism does not require surface tension. Instead, the selection comes about because the selected pattern is the only stable fixed point (attractor) of the non-singular bubble dynamics *without surface tension*.

Problem formulation and plan of the paper. A top-view of a Hele-Shaw channel with lateral walls at $y = \pm\pi$ in our scaled units and with the bubble moving to the right is shown on Fig. 1a. The fluid (oil) velocity obeys the 2D Darcy law, $\mathbf{v} = -\nabla p$, where p is scaled pressure. Far from the bubble the oil flows along the Ox axis with uniform velocity, $V = 1$, thus $p = -x$, when $|x| \rightarrow \infty$. Owing to incompressibility, $\nabla \cdot \mathbf{v} = 0$, p is harmonic, $\nabla^2 p = 0$, in the viscous domain, $D(t)$, where t denotes time. It is thus convenient to introduce a complex potential, $W = \Phi + i\Psi$, where $\Phi = -p$ and Ψ is the stream function. In view of the uniform far-field velocity, one has

$W = z$ for $|x| \rightarrow \infty$, so $\Psi = \pm\pi$ at $y = \pm\pi$, since the lateral walls are streamlines. Because pressure is constant (taken to be zero) in the inviscid bubble and continuous across the oil/bubble interface, $\Gamma(t)$, if surface tension is neglected, then $\Phi = 0$ at $\Gamma(t)$. The fluid domain in the W -plane is shown in Fig. 1b, where the vertical slit maps to the interface, $\Gamma(t)$, and the rest of the horizontal strip, $-\pi < \Psi < \pi$, to the domain, $D(t)$, in the physical plane (Fig. 1a). The kinematic identity, $V_n = v_n$, stating the equality of the normal velocities of the interface, V_n , and of the fluid, v_n , completes the formulation of this free-boundary problem of finding $\Gamma(t)$ given $\Gamma(0)$.

This long-standing nonlinear unstable problem [9] was shown to have an integrable structure and to possess deep connections with other branches of mathematical physics [10]. While numerous exact solutions were obtained for time-dependent interfaces (listed in [11]) and for steady shapes (see [12] and references therein), almost all of them were for singly-connected domains $D(t)$.

Here we present exact solutions for an evolving bubble in a Hele-Shaw cell when the fluid domain $D(t)$ is doubly connected (see Fig. 1a). We then show that these solutions explain not only *how* the moving bubble eventually

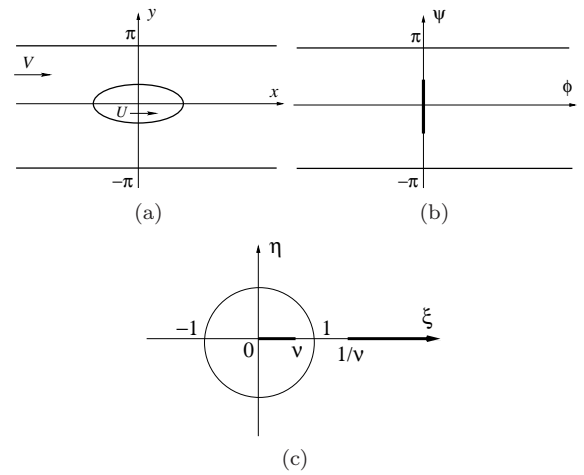


FIG. 1. The fluid domain $D(t)$ for a moving bubble in a Hele-Shaw channel (a), and the corresponding domains in the complex potential plane (b) and in the auxiliary ζ -plane (c).

reaches a stationary shape when $t \rightarrow \infty$, but also *why* the selected bubble moves precisely twice as fast (if to neglect surface tension) as the background flow [7].

In what follows, we first address the dynamics of a bubble with a shape symmetric with respect to the channel centerline. The exact solutions we obtain for this simpler case illustrate our main result, namely, that all non-singular solutions describing bubble shapes converge to the only stable fixed point of this infinitely-dimensional dynamical system, which is precisely the selected member of the continuous family [6]. After that, we extend our solutions to asymmetric bubbles and arrive at the conclusion that $U = 2$ is still the selected value.

The conformal map and the equation of motion. For a symmetric bubble we introduce a conformal map $z = f(t, \zeta)$ from the exterior of the unit circle with a cut in the complex plane, $\zeta = \xi + i\eta$ (see Fig. 1c), onto the fluid domain, $D(t)$ in the z -plane, $z = x + iy$. The unit circle, $|\zeta| = 1$, maps onto the interface, $\Gamma(t)$, and the cut sides, $\zeta = \xi \pm i0$, where $1 < 1/\nu(t) < \xi < \infty$, map onto the channel walls, $y = \pm\pi$, so that $\zeta = 1/\nu$ and $\xi = +\infty$ are mapped to $x = +\infty$ and $x = -\infty$, respectively. Thus, the polar angle $\phi = \arg(\zeta)$ parametrizes $\Gamma(t)$: $z = f(t, e^{i\phi})$. It is easy to see that the complex potential, $W = \Phi + i\Psi$, satisfying all aforementioned boundary conditions, is

$$W(t, \zeta) = \log \frac{1 - \nu/\zeta}{1 - \nu\zeta}. \quad (1)$$

Rewriting the normal velocity of the interface, V_n , as

$$V_n = V_1 l_2 - V_1 l_1 = \mathcal{I}m(\bar{V}l) = \mathcal{I}m(\bar{z}_t z_s),$$

where $l = l_1 + il_2 = dz/ds$ is the unit tangent vector along the interface, $\Gamma(t) = z(t, s)$, parametrized by an arclength, s , and the subscripts stand for partial derivatives. The normal fluid velocity we rewrite as

$$v_n = \partial_n \Phi = \partial_s \Psi,$$

by virtue of the Cauchy-Riemann condition. Equating the two last formulae, as required by the kinematic identity, and reparametrizing $s \rightarrow \phi$, we obtain $\mathcal{I}m(\bar{z}_t z_\phi) = \Psi_\phi$. Calculating Ψ_ϕ from (1) for $\zeta = e^{i\phi}$, we obtain the equation for the moving interface, $z(t, \phi) = f(t, e^{i\phi})$:

$$\mathcal{I}m(\bar{z}_t z_\phi) = \mathcal{R}e \frac{2\nu}{e^{i\phi} - \nu}. \quad (2)$$

For stationary solutions, $z(t, \phi) = Ut + Z(\phi)$, where the velocity, U , is a constant, equation (2) is simplified:

$$\mathcal{I}m(Z_\phi) = \frac{2\nu}{U} \mathcal{R}e \frac{1}{e^{i\phi} - \nu}. \quad (3)$$

The solution of (3) is the sum of two logarithms:

$$Z = -\log(1 - \nu e^{i\phi}) + \alpha \log(1 - \nu e^{-i\phi}), \quad (4)$$

where the coefficient at the first term equals 1 to satisfy $W = z$ in (1) when $z \rightarrow \infty$. Expression (4) is precisely

the one-parametric continuum of stationary bubbles obtained in [6]. Substituting (4) into (3), we obtain

$$U = \frac{2}{1 + \alpha}. \quad (5)$$

We will show that all solutions with $\alpha \neq 0$ are unstable, and, if perturbed, move to the solution with $\alpha = 0$. This will solve the selection of $U = 2$ in accordance with (5).

The finite-parametric solution. Being integrable, equation (2) possesses a rich list of exact solutions, and we found them. Many of these solutions blow up in finite time. Leaving those aside as physically non-realizable, we present here a rich class of finite-parametric *non-singular* solutions (analogous of those obtained earlier [13] for finger dynamics), which remain finite for all times:

$$z = \tau(t) - \log(1 - \nu(t)e^{i\phi}) + \sum_{k=0}^N \alpha_k \log(1 - a_k(t)e^{-i\phi}), \quad (6)$$

where $\alpha_0 = \alpha$ and τ are both real, $a_0 = \nu$, $|a_k| < 1$ for all times, and α_k are constants. These parameters must be chosen so that critical points of the conformal map always stay inside the unit circle to prevent blow ups [14]. Also, the symmetry of the bubble requires that for each term with complex α_k and a_k in the sum there is another term with $\bar{\alpha}_k$ and \bar{a}_k . It is easy to verify that (6) is indeed a solution of (2), where the time-dependence of τ , ν , and a_k is given by the following set of $N + 2$ equations:

$$\beta_k = \tau + \log \bar{a}_k / (\bar{a}_k - \nu) + \sum_{l=0}^N \alpha_l \log(1 - a_l \bar{a}_k), \quad (7a)$$

$$2t + 2t_0 = (1 + \alpha)\tau - \log(1 - \nu^2) + \sum_{k=1}^N \alpha_k \log(1 - \nu a_k), \quad (7b)$$

$$A = (|\alpha|^2 - 1) \log(1 - \nu^2) + \sum_{k=1}^N \sum_{l=1}^N \alpha_k \bar{\alpha}_l \log(1 - a_k \bar{a}_l), \quad (7c)$$

where $k = 1, \dots, N$ in (7a). Here the β_k , the initial time, t_0 , and the bubble area, A , are the constants of motion.

The attractor. It follows from (7b) and (7c) that $\tau(t)$ diverges linearly with time, $\tau \rightarrow Ut$, when $t \rightarrow +\infty$. Since β_k is a constant, a real part of at least one logarithm in (7a) should go to $-\infty$ in large times so as to compensate a divergent positive $\tau(t)$. This is possible only if all $a_k(t) \rightarrow 0$ for $k > 0$, as $t \rightarrow +\infty$. Thus, we conclude that the origin, $\zeta = 0$ attracts all $a_k(t)$ different from $\nu(t)$. But in this case the solution (6) approaches the family of stationary bubbles (4) discussed above, namely

$$z = \frac{2t}{1 + \alpha} - \log(1 - \nu e^{i\phi}) + \alpha \log(1 - \nu e^{-i\phi}),$$

which describes the selected value, $U = 2$, only if $\alpha = 0$.

If $a_0(0) = \nu(0)$ then $a_0(t) = \nu(t)$ for all times. To test the stability of the trajectory, $a_0(t) = \nu(t)$, one has to

deviate a little a_0 from ν . One can readily check that the dynamics of a_0 , ν and τ is given in this case by

$$\begin{aligned}\beta_0 &= \tau + \log \bar{a}_0 / (\bar{a}_0 - \nu) + \alpha \log[(1 - |a_0|^2)(1 - \bar{a}_0^2)], \\ 2(t + t_0) &= \tau - \log(1 - \nu^2) + \alpha \log |1 - a_0 \nu|, \\ A &= -\log(1 - \nu^2) + (\alpha^2/2) \log[(1 - |a_0|^2)|1 - \bar{a}_0^2|].\end{aligned}$$

These equations clearly show that $a_0 \rightarrow 0$, $\tau \rightarrow 2t$, and $\nu \rightarrow \sqrt{1 - e^{-A}}$ when $t \rightarrow \infty$, so the interface becomes

$$z = 2t - \log(1 - \nu e^{i\phi}). \quad (8)$$

This is precisely the selected pattern with $U = 2$. Thus, $\zeta = \nu$ repels nearly located singularities, which move toward 0. Therefore, the selected bubble, described by (8), represents the only attractor, $\zeta = 0$, of the non-singular subset of the finite-dimensional dynamical systems (6).

The infinitely-parametric solution. Let us extend (6) to the case of infinite number of parameters:

$$z = \tau(t) + \log \frac{1}{1 - \nu(t)e^{i\phi}} + \sum_{k=0}^N \int_0^{a_k(t)} \frac{\rho_k(t, w)}{w - e^{i\phi}} dw, \quad (9)$$

where $a_0 = \nu$ and $|a_k| < 1$ for all k . Solution (9) coincides with (6), if the functions $\rho_k(t, w)$ are constants, and contains all previously known solutions for single-connected and symmetric double-connected cases. (Apparently one can approximate any non-singular solution of (2) by (9), although we have not proved this.) The constants of motion for (9), analogous to β_k in (7), are $B_k = f(1/\bar{a}_k(t))$, which yield [15]

$$B_k = \tau(t) + \log \frac{\bar{a}_k(t)}{1 - \nu(t)\bar{a}_k(t)} + \sum_{l=0}^N \int_0^{a_l(t)} \frac{\rho_l(t, w)}{w - 1/\bar{a}_k(t)} d\zeta,$$

for $k = 1, \dots, N$. A proof, that τ diverges linearly with t , as $t \rightarrow \infty$, and testing the points, ν and 0, for stability is the same as above with the same conclusion that all $a_k \rightarrow 0$, implying that an arbitrary shape, expressed by (9), moves toward the selected bubble (8) with $U = 2$. After having analyzed symmetric bubbles, we now move on to the non-singular dynamics of non-symmetric bubbles.

Non-symmetric case. The complex potential for a non-symmetric shape requires infinity of reflected images, so we map conformally the annulus, $0 < \sqrt{q} < |\zeta| < 1$, in the ζ -plane (see Fig. 2) onto the fluid domain, $D(t)$, in the z -plane, so that the inner circle, $|\zeta| = \sqrt{q}$, is mapped onto the interface $\Gamma(t)$. The unit circle, $|\zeta| = 1$, is mapped onto the channel walls, $y = \pi$ and $y = 0$. Under reflection with respect to the unit circle (see Fig. 2), we obtain the pre-image of the domain, $\bar{D}(t)$, which is the complex conjugate of the $D(t)$. We map

$$\{\sqrt{q} < |\zeta| < 1/\sqrt{q}\} \rightarrow \{D(t) \cup \bar{D}(t)\},$$

where the annulus, $\sqrt{q} < |\zeta| < 1/\sqrt{q}$ is cut along the part of the unit circle, $0 < \arg \zeta < \gamma$, so that the inner (outer) cut side is mapped onto the north wall (its mirror

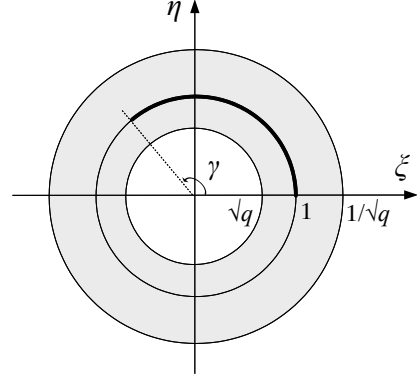


FIG. 2. Flow domain (shaded region) in the ζ -plane for an asymmetric bubble; see text.

image), where $y = \Psi = \pm\pi$, while the complimentary arc along the unit circle, $\gamma < \arg \zeta < 2\pi$, is mapped onto the south wall, where $y = \Psi = 0$. We fix the map by sending the points $\zeta = 1$ to $x = +\infty$ and $\zeta = e^{i\gamma}$ to $x = -\infty$.

The complex potential for the non-symmetric case is

$$W(\zeta) = i\gamma/2 + \log \frac{\Theta(e^{-i\gamma}\zeta) \Theta(q\zeta)}{\Theta(qe^{-i\gamma}\zeta) \Theta(\zeta)},$$

where

$$\Theta(\zeta) = (1-\zeta) \prod_{m=1}^{+\infty} (1-q^{2m}\zeta)(1-q^{2m}/\zeta) = \frac{\vartheta_4(\log(\sqrt{\zeta/q}), q)}{\prod_{m=1}^{+\infty} (1-q^{2m})},$$

$$\text{and} \quad \vartheta_4(w, q) = \sum_{n=-\infty}^{\infty} (-1)^n q^{n^2} \exp(2nw)$$

is the Jacobi theta function [16]. It is easy to verify that $W(\zeta)$ satisfies the boundary conditions indicated above.

Finite-parametric solutions in this case have the form

$$\begin{aligned}z(t, \phi) &= \tau(t) + i\gamma(t)/2 + \log \frac{\Theta(e^{i(\phi-\gamma(t))})}{\Theta(e^{i\phi})} + \\ &\sum_{k=1}^N [\alpha_k \log \Theta(a_k(t)e^{-i\phi}) + \bar{\alpha}_k \log \Theta(\bar{a}_k(t)e^{i\phi})].\end{aligned} \quad (10)$$

Here all $|a_k| < 1$, and $\sum_{k=1}^N \alpha_k = 0$. Since y is multiple of π , when $|\zeta| = 1$, then τ is purely real. Integrating the equations of motion, we obtain $N + 2$ complex constants of motion: $\beta_k = f(t, q/\bar{a}_k)$ for $k = 1, \dots, N$; $\beta_+ = f(t, q)$, and $\beta_- = f(t, qe^{i\gamma})$, where

$$\begin{aligned}\beta_k &= \tau + i\gamma/2 + \log [\Theta(qe^{i\gamma}\bar{a}_k)/\Theta(q\bar{a}_k)] + \\ &\sum_{l=1}^N [\alpha_l \log \Theta(a_l\bar{a}_k/q) + \bar{\alpha}_l \log \Theta(q\bar{a}_l/\bar{a}_k)],\end{aligned} \quad (11a)$$

$$\begin{aligned}\beta_{\pm} &= \tau - 2t + i\gamma/2 \pm \log [\Theta(qe^{i\gamma})/\Theta(q)] + \\ &\sum_{l=1}^N [\alpha_l \log \Theta(e^{-i\gamma\pm} a_l/q) + \bar{\alpha}_l \log \Theta(qe^{i\gamma\pm} \bar{a}_l)]\end{aligned} \quad (11b)$$

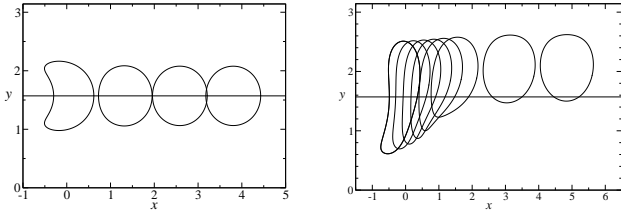


FIG. 3. Examples of bubble evolution: (a) symmetric solution and (b) asymmetric solution.

where $\gamma_+ = 1$ and $\gamma_- = \gamma$. The constants, β_+ and β_- are not independent, since $\text{Im} \beta_+ = \text{Im} \beta_- = \gamma/2 + \text{Im} \sum_{l=1}^N \alpha_l \log a_l$. The formulae (11) constitute the full dynamics of a_k , γ , q , and τ . The bubble area, A , while fixed in time, is not an independent constant of motion; it is neatly expressed through other constants as

$$A/\pi = \beta_+ - \beta_- + 2\text{Re} \sum_{k=1}^N \bar{\alpha}_k \beta_k.$$

The attractor. After eliminating τ , by subtracting β_{\pm} from β_k , we see at once from (11) that all $a_k \neq q$ move to the point $qe^{i\gamma}$, when $t \rightarrow \infty$. The ppoints q and $qe^{i\gamma}$ are the repeller and the attractor respectively for the dynamical system expressed by (11). Taken at the limit, $t \rightarrow \infty$, these two points are the only fixed points of this system. If one of a_k 's, say a_1 , was initially at the repeller, $a_1 = q$, then β_1 diverges, and $U = 2/(1 + \alpha_1) \neq 2$, when $t \rightarrow \infty$. After relocating a_1 out of q , the asymptotic velocity of the bubble eventually reaches the selected value, $U = 2$.

The solution (10) describes symmetric bubbles, when

$\beta = \pi$, thus (10) contains (6), albeit in a different formulation. A symmetric bubble evolution is shown in Fig. 3a, where the asymptotic shape corresponds to the Taylor-Saffman bubble [6] with $U = 2$, as described by (8). In Fig. 3b we show an asymmetric solution whose steady shape (reached in the long-time limit) corresponds to the Tanveer asymmetric bubble [8, 12] with $U = 2$.

Final remarks:

(i) Since all a_k move toward the same point, $a_k \rightarrow qe^{i\gamma}$, for $t \rightarrow \infty$, the sum in (11) vanishes, because $\sum_{k=1}^N \alpha_k = 0$, so $\gamma(t) \rightarrow \text{Im} \beta_+ = \text{Im} \beta_-$, which, being a constant of motion, can be any number chosen freely at $t = 0$. Thus, it remains to be seen how to centralize a bubble in our framework (if possible at all), so that $\gamma \rightarrow \pi$ as $t \rightarrow \infty$.

(ii) We do not present here the $U = 2$ selection for the asymmetric bubble with infinitely-parametric non-singular solutions, that is the analog of (9) but with use of theta-functions. While the algebra is lengthy, the result is the same, $U = 2$, in the limit $t \rightarrow \infty$, as expected.

(iii) Presented results (and the result of [5], which is a singular limit of this work: $\nu \rightarrow 1 + \epsilon$, for $0 < \epsilon \ll 1$) unambiguously indicate that stability of the selected pattern, with respect to the rest of the family, is built in the Laplacian growth *without surface tension*. Surface tension is just one of infinitely many perturbations (perhaps the most relevant), which kicks the system toward the attractor, while also regularizing high curvatures.

(iv) The selected pattern, while linearly unstable, is stable asymptotically: if perturbed, it eventually recovers its original shape. It is tempting to regularize our theory (by means of surface tension or otherwise) and to see which subset of the presented solutions will survive.

One of the authors (M.M-W) would like to thank the Max Planck Institute for Complex Systems (Dresden) for hospitality during preparation of the part of this work.

-
- [1] G. P. Ivantsov, Dokl. Akad. Nauk. SSSR bf 58, 567 (1947).
 - [2] P.G. Saffman and G. I. Taylor, Proc. R. Soc. Lond. A **245**, 312 (1958).
 - [3] P. Pelcé, *Dynamics of Curved Fronts* (Academic Press, San Diego, 1988).
 - [4] B.I. Shraiman, Phys. Rev. Lett. **56**, 2028 (1986); D.C. Hong and J.S. Langer, Phys. Rev. Lett. **56**, 2032 (1986); R. Combescot et al., Phys. Rev. Lett. **56**, 2036 (1986); S. Tanveer, Phys. Fluids **30**, 1589 (1987).
 - [5] M. Mineev-Weinstein, Phys. Rev. Lett. **80**, 2113 (1998).
 - [6] G. I. Taylor and P. G. Saffman, Q. J. Mech. Appl. Maths **12**, 265–279 (1959).
 - [7] A. R. Kopf-Sill and G. M. Homsy, Phys. Fluids **31**, 18 (1988), T. Maxworthy, J. Fluid Mech. **173**, 95 (1986). S. Shad et al., J. of Petrol. Sci. and Eng. **72**, 67–77 (2010).
 - [8] S. Tanveer, Phys. Fluids **30**, 651 (1987)
 - [9] A comprehensive bibliography on the subject up to 1998: <http://people.maths.ox.ac.uk/howison/Hele-Shaw>.
 - [10] M. Mineev-Weinstein, P. B. Wiegmann, and A. Zabrodin, Phys. Rev. Lett. **84**, 5106 (2000).
 - [11] B. Gustafsson and A. Vasil'ev, *Conformal and Potential Analysis in Hele-Shaw Cell* (Birkhäuser, Basel, 2006); M. Mineev-Weinstein, M. Putinar, R. Teodorescu, J. Phys. A **41** 263001 (2008).
 - [12] G. L. Vasconcelos, J. Fluid Mech. **444**, 175 (2001).
 - [13] M. Mineev-Weinstein and S. P. Dawson, Phys. Rev. E **50**, R24 (1994); S. P. Dawson and M. Mineev-Weinstein, Physica (Amsterdam) **73D**, 373 (1994).
 - [14] One should also stay away from initial data leading to the loss of univalence of the interface. It is easy to accommodate, and we do not discuss details here.
 - [15] The rest of formulae related to the solution (9) will be presented elsewhere.
 - [16] I. S. Gradshteyn and I. M. Ryzhik, Table of Integrals, Functions, and Products, (1980) Acad. Press, London.